

# Scalable Change Retrieval Using Deep 3D Neural Codes

Kojima Yusuke    Tanaka Kanji    Yang Naiming    Hirota Yuji

## Abstract

We present a novel scalable framework for image change detection (ICD) from an on-board 3D imagery system. We argue that existing ICD systems are constrained by the time required to align a given query image with individual reference image coordinates. We utilize an invariant coordinate system (ICS) to replace the time-consuming image alignment with an offline pre-processing procedure. Our key contribution is an extension of the traditional image comparison-based ICD tasks to setups of the image retrieval (IR) task. We replace each component of the 3D ICD system, i.e., (1) image modeling, (2) image alignment, and (3) image differencing, with significantly efficient variants from the bag-of-words (BoW) IR paradigm. Further, we train a deep 3D feature extractor in an unsupervised manner using an unsupervised Siamese network and automatically collected training data. We conducted experiments on a challenging cross-season ICD task using a publicly available dataset and thereby validate the efficacy of the proposed approach.

## I. INTRODUCTION

Recent progress in simultaneous localization and mapping (SLAM) has led to the development of various practical SLAM systems (e.g., LSD-SLAM [1]) that can map large environments via egocentric on-board 3D vision (e.g., 3D LIDAR imagery). However, SLAM in non-stationary environments remains a significant challenge [2]–[5]. A major source of difficulty is the large number of possible changes between live images and a map (e.g., of car parking and building construction), which grows combinatorially relative to the map size. To reduce computational and perceptual complexity, it is helpful if an SLAM system has the ability of detecting changed objects.

The detection of changed objects in a query live image relative to a pre-built background model (i.e., a map) is a fundamental problem in computer vision called image change detection (ICD) [6], which has been studied in many different contexts, including remote sensing [7] and surveillance [8]. In these classical contexts, the problem is typically formulated as a two-stage image comparison process. The first stage, alignment, is aimed to align the query image with the reference image coordinate system. The second stage, differencing, is aimed to compare the query and reference images with respect to the reference coordinate system. However, this two-stage process requires a large number of alignment and differencing operations for every possible reference image, the time cost of which is prohibitive for time-critical vehicular applications.

We were particularly interested in the use of the viewpoint invariant coordinate system (ICS) [9], which solves the above problems, and this motivated our study. Our approach integrates the alignment and differencing steps in a unique manner. Our key idea is to align an input query image with a pre-defined ICS, rather than to align it with individual reference images. This allows the image alignment to be a part of the offline pre-processing, which leads to a significant reduction in online processing [10].

The main contribution of this paper is an extension of the traditional image comparison task to setups of the image retrieval task (Fig. 1). More formally, we replace each component of the 3D ICD system, i.e., (1) image modeling, (2) image alignment, and (3) image differencing, with significantly efficient variants from the bag-of-words (BoW) image retrieval paradigm [11]. Our BoW-based approach was primarily motivated by two independent fields: viewpoint-localization (VL) [12] and ICD [13], in which codeword (i.e., BoW) models are used as compact appearance models based on vector quantization. Our key contribution is that the advantages of the two independent BoW techniques are combined into a unified change retrieval (CR) framework. We introduce the ICS mentioned above to allow the direct comparison of appearance features in the query and reference images without the online pre-alignment step. Further, we train a deep 3D feature extractor in an unsupervised manner using an unsupervised Siamese network and a weakly labeled training set automatically collected from the target environments. The result is an extremely efficient deep CR framework that requires only a single look-up of the inverted file and a few L2 norm comparisons. The results of experiments on a challenging cross-season CR (CS-CR) task using the North Campus Long-Term (NCLT) dataset [14] validate the feasibility of the proposed method.

## II. APPROACH

The objective of CR is to detect a significant change between query and reference images that are observed at different times. A query image is modeled as a local point-cloud (PC) map, which is built from a sequence of sensor data acquired by a vehicle’s on-board 3D scanner during short-range navigation. A reference image is modeled by a local PC image in the same format. Each short sequence corresponds to the vehicle’s travel distance of 5 m. A local map is constructed by aligning this short sequence of 3D scans. The alignment is based on dead-reckoning, inertial measuring units, and an iterative closest point (ICP) algorithm.

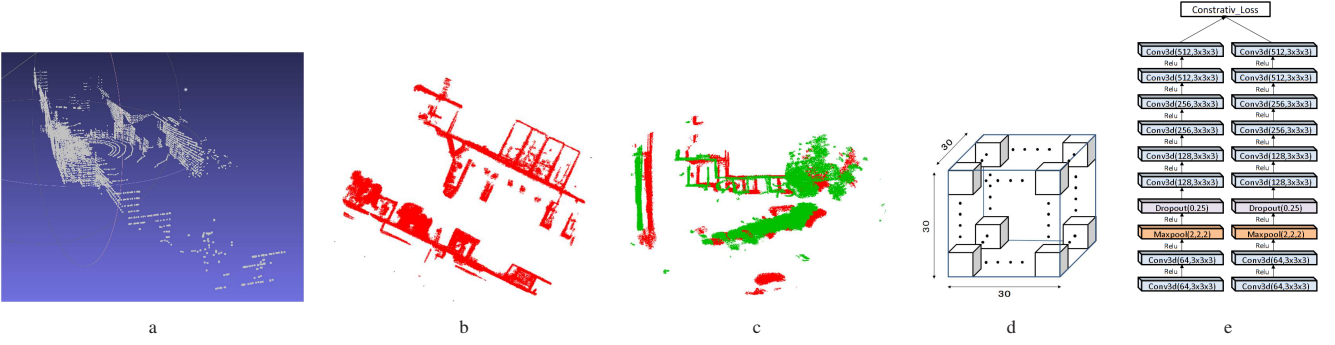


Fig. 1. Proposed framework. (a) A short sequence of 3D scans is acquired by the on-board imagery. (b) A 3D image (local map) is built by aligning scans in the input sequence. (c) Every query/reference image is aligned with the invariant coordinate system to allow direct comparison of the 3D keypoints. (d) A constant-dimensional truncated distance function (TDF) vector is obtained from each of the local interest regions in a query/reference image. (e) A Siamese network is trained from weakly labeled TDF vector pairs to learn discriminative 3D neural codes.

We followed studies in the literature [6] to formulate the CR task as a task consisting of localizing change objects with respect to the environment. Unlike many other applications, vehicular applications cannot always assume the availability of precise viewpoint information. For example, GPS is frequently occluded by trees, terrain, or buildings. Therefore, we must consider the task of joint viewpoint-change localization under global viewpoint uncertainty [9].

The performance of a retrieval task is frequently evaluated by a ranking-based metric. In this study, we employed two different such metrics, averaged normalized rank (ANR) [15] and top- $X$  accuracy [16], for the VL and ICD tasks, respectively. ANR utilizes a ranked list of viewpoints in descending order of relevance score. It is defined as the average of the ranks of the ground-truth viewpoint normalized by the database size. Top- $X$  accuracy utilizes a collection of top- $X$  datapoints with the highest likelihood of change (LoC) and is defined as the ratio of query images where ICD is successful. The success of ICD is defined by whether the ground-truth bounding boxes (of changed objects) overlap with the top- $X$  ranked datapoints.

The proposed CR framework consists of offline and online processes. Offline, a discriminative feature extractor is trained in an unsupervised manner (Section II-A) from a weakly-labeled training set. Online, first each of the images is converted to a collection of local features (Section II-A), and then, their appearance descriptors are translated to the compact BoW representation (Section II-B), while their 3D keypoints are transformed to ICS (Section II-C). Then, VL (Section II-D) and ICD (Section II-E) are performed based on the BoW and ICS formulations. These processes are detailed in the following subsections.

### A. Three-dimensional Deep Neural Codes

The feature extractor is aimed to extract a collection of local features from a given query/reference image. This task consists of three stages. First, a collection of  $N = 500$  is sampled from the PC. Then, the local interest region of each keypoint is translated to a  $30^3$  dimension vector by the truncated distance function (TDF) [17]. Finally, the TDF vector is translated to a 512-dim discriminative feature vector by a convolutional neural network (CNN). The TDF and CNN are detailed in the following.

The TDF is a technique for translating variable size PC data to a constant dimension vector representation. This constant dimension vector representation is useful for inputting data to a CNN, as most state-of-the-art CNNs are based on the assumption of a constant dimension input. In our approach, a size  $30 \times 30 \times 30$  voxel grid is imposed within a given  $9 \times 9 \times 9$  [ $m^3$ ] interest region, and the local PC in each voxel is approximated by its TDF value, which yields a  $30^3 = 27,000$  dimensional vector.

The CNN is pre-trained in an unsupervised manner by using a Siamese network. A Siamese network is a Y-shaped neural network that joins two network branches in the final layers to produce a single output. The two branches have the same layer structure. The network is trained in a weakly-supervised scheme for learning a similarity measure from training samples of similar/dissimilar TDF vector pairs. Each branch is a CNN with eight 3D convolutional layers. These layers have different numbers of kernels of 64-64-128-128-256-256-512-512 with a kernel size of  $3 \times 3$ . A max-pooling layer with a pool size of  $2 \times 2 \times 2$  and a dropout layer of ratio 0.25 are inserted after the second convolutional layers. Inspired by [17], we consider the trained CNN a discriminative feature extractor and use it as a feature extractor for converting a given TDF vector to a 512 dimensional feature vector. We extend the framework of [17] from indoor RGB-D data to outdoor 3D scanner data.

The training data for the feature extractor can be automatically collected by the vehicle itself in the target domain. A collection of similar/dissimilar TDF vector pairs is required as positive/negative training data for the Siamese network. The positive samples are defined as TDF vector pairs (from the training sequence) in two different viewpoints originating from the same real-world object. The negative samples are the other majority of TDF vector pairs. Therefore, negative samples can

TABLE I  
PERFORMANCE RESULTS.

	VL	ICD	
		w/o ICS	w/ ICS
FPFH	15.1	-	-
Siamese	10.8	-	-
FPFH-BoW	39.3	32.9	52.1
Siamese-BoW	13.1	71.0	83.0

be easily sampled from the TDF vector pairs. However, the automatic collection of positive pairs is not a trivial task. In this study, we employed a two stage approach. First, relative localization between two successive local PC images at time stamp  $t$  and  $t + 3$  [sec] within the training sequence is performed by using the available dead-reckoning measurements. Second, fine-grained registration is performed using the ICP as described in [18]. Then, the two aligned PCs are both cropped by the same bounding box of size  $0.3 \times 0.3 \times 0.3 \text{ m}^3$  at the interest region to obtain paired TDF vectors. It is noteworthy that the above procedure is fully automatic and does not require human intervention.

### B. Bag of Words Representation

Local features in query/reference images are encoded to the BoW representation. Formally, each local feature is vector quantized and encoded to visual word  $w \in [1, W]$  ( $W = 10,000$ ). This is equivalent to the task of finding the nearest neighbor (NN) exemplar in a pre-defined collection of exemplar features called a vocabulary, and the ID of the NN exemplar is defined as the visual word. Then, the visual word can be used as a compact index for efficient image retrieval. For the vocabulary, a classifier with  $W$  clusters is pretrained offline using the unsupervised k-means clustering algorithm presented in [19]. The training image for the classifier is a size 1.2M collection of local features (from 2,409 images), which is independent of the training/testing data used for experiments.

### C. Invariant Coordinate System (ICS)

The keypoints of each local feature in each query/reference image are transformed to the ICS [9]. The ICS should be designed to be invariant to the vehicle viewpoints, to allow direct comparison of the keypoints of local features in different 3D images under viewpoint uncertainty. It is noteworthy that online alignment is required only for the query image. The alignment for reference images can be accomplished offline, which leads to a significant reduction in online computation.

A key design issue is the determination of the origin and axes of the ICS [10]. In this study, we assumed that the vertical axis of the image coordinate is known and orthogonal to the horizontal ground plane. For determining the two horizontal coordinate axes, we adopted the entropy minimization criteria described in [20]. For determining the origin, we adopted a strategy called “center-of-gravity (CoG)”, which determines the origin as the centre of gravity of the given PC. The CoG strategy was proposed in our previous paper [21], further verified in [22], and successfully applied in tasks on VL [23] and ICD [10]. Moreover, the current paper also describes an ablation study to verify the effectiveness of ICS in our novel CR task.

### D. Viewpoint Localization

3D BoW features are fed to a standard VL algorithm, in which the NN reference image  $j$  is determined by minimizing the naive Bayes nearest neighbor (NBNN) distance metric:

$$j = \arg \min_j \sum_{q \in Q} \min_{r \in R_j} |q - E(r)|. \quad (1)$$

$|\cdot|$  is L2 norm.  $Q$  and  $R_j$  are the collections of features from the query and the  $j$ -th reference image, respectively.  $q$  is a raw feature vector in the query image.  $E(r)$  is an exemplar that corresponds to the visual word of interest and approximates the reference feature vector  $r$  (Section II-B) that corresponds to the visual word of interest.

### E. Image Change Detection

The relevant reference images hypothesized by the VL are compared to a query image in terms of appearance and spatial cues. Appearance cues are the BoW representations that are extracted by a discriminatively trained CNN (Section II-A) and further encoded to the BoW-based representation (Section II-B). Spatial cues are the 3D keypoints that are based on ICS (Section II-C). Based on these appearance and spatial cues, the LoC of a datapoint in a given query image is defined as the L2 distance to the NN reference image in the feature space. Following [24], its search region for the NN reference feature is defined as a horizontal bounding box in ICS. The horizontal plane is partitioned at  $x=0, \pm \bar{x}$  on  $x$ -axis and at  $y=0, \pm \bar{y}$  on  $y$ -axis, into  $4 \times 4$  grid cells and those cell which the query keypoint belongs to is considered the local search region.  $\bar{x}$  and  $\bar{y}$  are means of the absolute values of the  $x$  and  $y$  of all the datapoints in the training images.

### III. EXPERIMENTS AND DISCUSSIONS

We evaluated the suitability of the methods presented above for CS-CR using the NCLT dataset [14].

This dataset is a long-term autonomy dataset for robotics research collected at the University of Michigan's North Campus. The dataset consists of omnidirectional imagery, 3D LIDAR, planar LIDAR, GPS, and odometry data. During vehicle travel in outdoor environments, various types of appearance changes were encountered with respect to the data from different seasons. These changes originate from the movement of people, parked cars, building construction, and other nuisance changes originating from viewpoint-dependent changes of object appearances and occlusions, weather changes, falling leaves, and snow. These appearance changes make our CS-CR task challenging.

We utilized the PC data from the LIDAR as input to our CS-CR tasks. We used the available GPS information only as the ground-truth data. We used datasets of four different seasons, where the images were captured on "2012/3/31 (SP)," "2012/8/04 (SU)," "2012/11/17 (AU)," and "2012/1/22 (WI)," as individual training/testing sets. As aforementioned, we did not assume the availability of ground-truth viewpoint information, and considered multiple candidates of relevant reference images. The numbers of these reference image candidates were 130, 116, 121, and 133 for SP, SU, AU, and WI.

We created an image set consisting of 100 query images. More specifically, we considered all the 12 different combinations of query-reference dataset seasons. Each query image belonged to a different season's dataset from those of the reference images. In each selected query image, the ground-truth GPS locations of the two images were sufficiently close and newly appearing change objects (e.g., parking cars) were present with respect to the relevant reference image. We annotated the changed objects in the query image by 2D bounding boxes on the horizontal plane. We compared the proposed ICD algorithm using deep neural codes with an alternative algorithm based on the fast point feature histogram (FPFH) presented in [25].

Table I shows the ICD performance in terms of top- $X$  accuracy. The proposed method frequently successfully aligned the invariant coordinate system of the query and the reference images. This allowed the spatial information of local features with respect to the coordinate systems to be utilized as an additional discriminative cue for VL. The proposed method clearly outperforms the baseline FPFH method.

### REFERENCES

- [1] J. Engel, T. Schöps, and D. Cremers, "Lsd-slam: Large-scale direct monocular slam," in *European Conference on Computer Vision*. Springer, 2014, pp. 834–849.
- [2] M. J. Milford and G. F. Wyeth, "Seqslam: Visual route-based navigation for sunny summer days and stormy winter nights," in *Robotics and Automation (ICRA), 2012 IEEE International Conference on*. IEEE, 2012, pp. 1643–1649.
- [3] W. Churchill and P. Newman, "Experience-based navigation for long-term localisation," *The International Journal of Robotics Research*, vol. 32, no. 14, pp. 1645–1661, 2013.
- [4] M. Paton, K. MacTavish, M. Warren, and T. D. Barfoot, "Bridging the appearance gap: Multi-experience localization for long-term visual teach and repeat," in *Intelligent Robots and Systems (IROS), 2016 IEEE/RSJ International Conference on*. IEEE, 2016, pp. 1918–1925.
- [5] B. Mathias, D. Marcin, G. Igor, C. Cesar, S. Roland, and N. Juan, "Map management for efficient long-term visual localization in outdoor environments," in *Intelligent Vehicle Symposium, IEEE*, 2018.
- [6] R. J. Radke, S. Andra, O. Al-Kofahi, and B. Roysam, "Image change detection algorithms: a systematic survey," *IEEE transactions on image processing*, vol. 14, no. 3, pp. 294–307, 2005.
- [7] L. Gueguen and R. Hamid, "Large-scale damage detection using satellite imagery," in *Proceedings of the IEEE Conference on Computer Vision and Pattern Recognition*, 2015, pp. 1321–1328.
- [8] W. Sultani, C. Chen, and M. Shah, "Real-world anomaly detection in surveillance videos," *Center for Research in Computer Vision (CRCV), University of Central Florida (UCF)*, 2018.
- [9] Y. Takahashi, K. Tanaka, and N. Yang, "Scalable change detection from 3d point cloud maps: Invariant map coordinate for joint viewpoint-change localization," in *21st International Conference on Intelligent Transportation Systems, ITSC 2018, Maui, HI, USA, November 4-7, 2018*, 2018, pp. 1115–1121. [Online]. Available: <https://doi.org/10.1109/ITSC.2018.8569294>
- [10] —, "Scalable change detection from 3d point cloud maps: Invariant map coordinate for joint viewpoint-change localization," in *Intelligent Transportation Systems (ITSC), 2018 IEEE 21th International Conference on*, 2018.
- [11] Z. S. Harris, "Distributional structure," *Word*, vol. 10, no. 2-3, pp. 146–162, 1954.
- [12] M. Cummins and P. M. Newman, "Appearance-only SLAM at large scale with FAB-MAP 2.0," *I. J. Robotics Res.*, vol. 30, no. 9, pp. 1100–1123, 2011.
- [13] K. Kim, T. H. Chalidabhongse, D. Harwood, and L. Davis, "Real-time foreground-background segmentation using codebook model," *Real-time imaging*, vol. 11, no. 3, pp. 172–185, 2005.
- [14] N. Carlevaris-Bianco, A. K. Ushani, and R. M. Eustice, "University of michigan north campus long-term vision and lidar dataset," *The International Journal of Robotics Research*, pp. 1023–1035, 2015.
- [15] M. Ando, Y. Chokushi, K. Tanaka, and K. Yanagihara, "Leveraging image-based prior in cross-season place recognition," in *IEEE International Conference on Robotics and Automation, ICRA 2015, Seattle, WA, USA, 26-30 May, 2015*, 2015, pp. 5455–5461. [Online]. Available: <https://doi.org/10.1109/ICRA.2015.7139961>
- [16] S. Ren, K. He, R. Girshick, and J. Sun, "Faster r-cnn: Towards real-time object detection with region proposal networks," in *Advances in neural information processing systems*, 2015, pp. 91–99.
- [17] A. Zeng, S. Song, M. Nießner, M. Fisher, J. Xiao, and T. Funkhouser, "3dmatch: Learning local geometric descriptors from rgb-d reconstructions," in *CVPR*, 2017.
- [18] P. J. Besl and N. D. McKay, "Method for registration of 3-d shapes," in *Sensor Fusion IV: Control Paradigms and Data Structures*, vol. 1611. International Society for Optics and Photonics, 1992, pp. 586–607.
- [19] J. MacQueen *et al.*, "Some methods for classification and analysis of multivariate observations," in *Proceedings of the fifth Berkeley symposium on mathematical statistics and probability*, vol. 1, no. 14. Oakland, CA, USA, 1967, pp. 281–297.
- [20] S. Olufs and M. Vincze, "Robust single view room structure segmentation in manhattan-like environments from stereo vision," in *2011 IEEE International Conference on Robotics and Automation*. IEEE, 2011, pp. 5315–5322.
- [21] H. Shogo and T. Kanji, "M2t: Local map descriptor," in *2014 IEEE/SICE International Symposium on System Integration*, Dec 2014, pp. 210–215.

- [22] E. Liu, K. Tanaka, and X. Fei, "Grammar-based map parsing for view invariant map descriptor," in *2017 International Conference on Indoor Positioning and Indoor Navigation, IPIN 2017, Sapporo, Japan, September 18-21, 2017*, 2017, pp. 1–8. [Online]. Available: <https://doi.org/10.1109/IPIN.2017.8115884>
- [23] Y. Takahashi, K. Tanaka, and Y. Fang, "Cross-season vehicle localization using bag of local 3d features," in *20th IEEE International Conference on Intelligent Transportation Systems, ITSC 2017, Yokohama, Japan, October 16-19, 2017*, 2017, pp. 1–6. [Online]. Available: <https://doi.org/10.1109/ITSC.2017.8317606>
- [24] S. Lazebnik, C. Schmid, and J. Ponce, "Beyond bags of features: Spatial pyramid matching for recognizing natural scene categories," in *2006 IEEE Computer Society Conference on Computer Vision and Pattern Recognition*, 2006, pp. 2169–2178.
- [25] R. B. Rusu, N. Blodow, and M. Beetz, "Fast point feature histograms (fpfh) for 3d registration," in *2009 IEEE International Conference on Robotics and Automation*. IEEE, 2009, pp. 3212–3217.